

Effect of Zone Annealing on LARC-CPI Thermoplastic Polyimide

JUSTYNA B. TEVEROVSKY,* DAVID C. RICH, YOSHIHIKO AIHARA,[†] and PEGGY CEBE[‡]

Department of Materials Science and Engineering, Massachusetts Institute of Technology, Cambridge, Massachusetts 02139

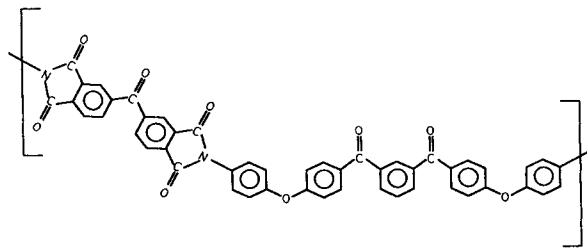
SYNOPSIS

Mechanical properties and structure were studied for undrawn and zone-drawn films of LARC-CPI thermoplastic polyimide. The dynamic modulus of undrawn glassy material ranged from about 1.8 to 4.3 GPa, depending upon the degree of crystallinity. After zone drawing to draw ratios of 3.6–4.0, the dynamic glassy modulus was increased to a maximum of 9.5 GPa. The highest moduli were attained in samples that were multiply zone-drawn. The maximum-achievable draw ratio increased with the maximum drawing temperature, but the semicrystalline nature of the starting material limited the ultimate drawability. For the first time, highly oriented crystalline films were obtained for X-ray diffraction and preliminary crystal structure analysis. The crystal lattice was fit to the orthorhombic crystal system, and the results indicate that the lattice parameters are $a = 8.0 \pm 0.2 \text{ \AA}$, $b = 5.9 \pm 0.2 \text{ \AA}$, and $c = 36.5 \pm 0.3 \text{ \AA}$. The value of the c -axis lattice parameter is very close to the fully extended chain length of the monomer repeat unit. © 1994 John Wiley & Sons, Inc.

INTRODUCTION

As part of our overall effort in high-performance polymers, our group has been studying structure–property relationships in several semicrystalline thermoplastic polyimides, including Regulus NEW-TPI^{1–7} and LARC-CPI.^{5–11} The latter polymer, a product of the NASA Langley Research Center,^{12–16} is the subject of the present study, which was to apply the technique of zone drawing^{17–28} to achieve improvement in amorphous- and crystal-phase orientation. Previously, we applied zone drawing to amorphous NEW-TPI films^{1,2} and their blends with Xydar liquid crystalline polymer.^{2,3} In that work, by drawing above the T_g , we were able to achieve significant draw ratios, near 8.0, but the glassy modulus was not substantially altered by the drawing treatment.^{1–3}

Previous researchers used the technique of zone annealing to draw thermoplastic polymers that were already once-drawn and, hence, oriented and semicrystalline.^{17–22} Here, we apply the zone-annealing treatment to undrawn, but semicrystalline, films of LARC-CPI. This polyimide is formed from the reaction of 3,3',4,4'-benzophenonetetracarboxylic dianhydride (BTDA) with 1,3-bis(4-aminophenoxy-4'-benzoyl)benzene (1,3-BABB). The chemical structure has been reported previously,^{12–16} as well as its crystallization behavior and morphology.^{29–32} The monomer unit of LARC-CPI is shown below:



The present study had two purposes: First, we wanted to evaluate the ability of semicrystalline films of LARC-CPI to be drawn using the zone-annealing treatment. We found that network extension

* Present address: Foster Miller, Inc., Waltham, MA.

[†] Present address: Showa Shell Chemical Company, Tokyo, Japan.

[‡] To whom correspondence should be addressed.

in this material is limited by the reinforcing effect of the crystal phase. Upon heating the oriented zone-drawn material, we found that there was a large component of elastic recovery within the amorphous phase. Thus, the glassy modulus was not stable when the films were heated. Second, it was our goal to obtain highly oriented semicrystalline films that could be used in X-ray scattering studies to elucidate the crystal structure, which has not yet been reported for this polymer. We found that the fiber X-ray patterns of oriented LARC-CPI displayed orthorhombic symmetry, and the lattice parameters were determined.

EXPERIMENTAL

Materials and Characterization

Solution-cast films of LARC-CPI were provided by Dr. Terry St. Clair of the NASA Langley Research Center. Polyamic acid precursor was cast on glass and thermally converted to polyimide by treating for 1 h at 100, 200, and, finally, 300°C. Comparison of the infrared spectral bands at 1775 cm^{-1} (imide) and 1640 cm^{-1} (amide) to the benzene ring absorption at 1491 cm^{-1} revealed that the as-received films were completely imidized.⁸ The films were translu-

cent yellow and had a thickness of 0.065 mm. Examination by wide-angle X-ray scattering (WAXS) and by optical microscopy between crossed polarizers revealed no orientation in the plane of the film.

Films were examined using a Perkin-Elmer DSC-4 differential scanning calorimeter (DSC), calibrated using indium. In Figure 1, thermograms of as-received (AR) film (curve 1) and two zone-drawn films (curves 2 and 3) are shown. The zone-drawn films will be discussed in more detail later. The thermogram of the AR film (curve 1) is similar to that shown previously,⁹ but this film had a higher degree of crystallinity than that of the previous film,⁹ with a degree of crystallinity, χ_c , about 0.40 by weight compared to 0.24 in the prior study.⁹ Crystallinity was determined using 92 J/g as the heat of fusion of the perfect crystalline form.⁹ The glass transition temperature ranges from about 222°C for amorphous LARC-CPI to 230°C for the semicrystalline material. The melting endotherm is very broad and peaks at about 360°C. For the AR films, no additional crystallization occurs upon heating in the DSC above the glass transition temperature. Another film was studied for comparison: AR film was melted at 400°C briefly, then quenched to obtain amorphous material. This film will be referred to as QA.

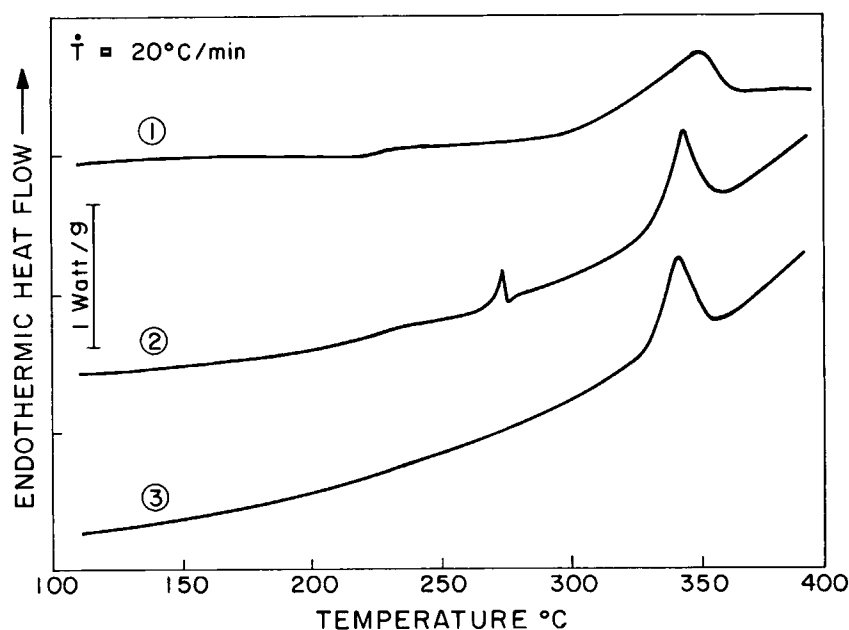


Figure 1 DSC thermograms of LARC-CPI at 20°C/min scan rate for as-received film (curve 1), film zone-annealed to draw ratio 3.88 (curve 2), and film zone-annealed to draw ratio 3.88 and then relaxed by heating to 300°C (curve 3). Curves are normalized to the same unit mass and are vertically displaced for clarity. The vertical scale bar represents a heat flow of 1 mW/mg.

Mechanical properties of the LARC-CPI films were measured using a Seiko DMS 200 in the tension mode. Measurements were made from 0 to 350°C, or to failure, by heating at 2°C/min. Measurement frequencies were 1, 2, 5, 10, or 20 Hz. Two-dimensional X-ray patterns were recorded on Kodak DEF5 film using a Statton camera with sample-to-film distances of about 3 cm (WAXS) and 13 cm (SAXS, small-angle X-ray scattering). The X-ray source was a Philips PW1830 generator with nickel-filtered $\text{CuK}\alpha$ radiation, operated at 45 kV and 45 mA. Exposure times were on the order of 10 h (WAXS) to 24 h (SAXS). The silicon powder standard from the National Institute of Standards and Technology was rubbed on the film surface for calibration of the sample-to-film distances.

Zone Annealing

The apparatus used to form oriented films is a zone-drawer described previously.¹⁻³ The zone-drawer consists of a heater with a 2 mm wide slot through it. The heater temperatures we used were 250, 265, 280, 295, and 310°C. A strip of LARC-CPI AR film 5 mm wide and 8 cm long is threaded through the heater slot at room temperature. The heater does not come in contact with the film during drawing. The heated slot moves along the film in one direction at a fixed speed of 1 cm/min while a tension force pulls the film in the opposite direction. The tension force is applied by dead weights, which ranged in mass from 500 to 1200 g. Fiduciary marks on the film surface allow determination of extension ratio, λ ($\lambda = \text{final length}/\text{original length}$), after drawing. The design of the zone-drawer follows that described by other researchers.^{27,28}

As defined by Kunugi et al.,¹⁷⁻²² zone drawing (ZD) and zone annealing (ZA) are distinguished by the temperature used for drawing. Zone drawing is carried out between the glass transition temperature and the crystallization temperature, usually on originally amorphous films. Zone annealing is performed between the crystallization temperature and the melting point, usually on crystalline films. All the drawings performed in this study are classified as zone annealing.

RESULTS AND DISCUSSION

Mechanical Properties of Undrawn LARC-CPI

Figure 2 shows the dynamic mechanical analysis of the LARC-CPI films from 50 to 350°C. The AR film is shown in Figure 2(a) with storage modulus and

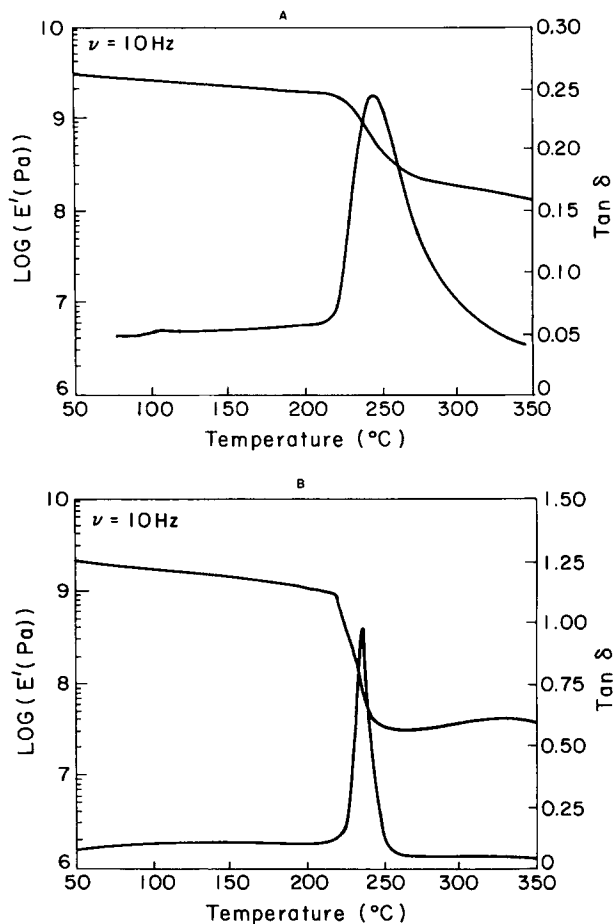


Figure 2 Dynamic mechanical properties, E' and $\tan \delta$, of LARC-CPI as a function of temperature, at 10 Hz: (a) as-received film; (b) quenched amorphous film.

$\tan \delta = E''/E'$ displayed on the left and right vertical axes, respectively. The QA film is shown in Figure 2(b). Nothing unusual was seen as a function of frequency, so only the 10 Hz data are shown in Figure 2. Each material shows a glassy region ($T < 200^\circ\text{C}$), a transition region ($200^\circ\text{C} < T < 250\text{--}275^\circ\text{C}$), and a rubbery region ($T > 250\text{--}275^\circ\text{C}$). These temperature ranges are approximate and vary depending upon whether the film is semicrystalline or amorphous. The glassy modulus at 50°C is 3.0 GPa for AR and 2.0 GPa for QA. For a total of 20 AR films studied, the room temperature value of the storage modulus ranged from 1.8 to 4.3 GPa.

There is temperature dependence of the glassy modulus, which drops steadily from room temperature to about 210°C, at which point the glass transition relaxation sets in. AR ($\chi_c = 0.40$) has a broad glass transition region over which E' declines by about one decade. The $\tan \delta$ peak covers a 90°C

spread and has a small peak amplitude. In contrast, the QA sample shows a very steep drop in E' by nearly two decades, within a narrow range of about 30°C. The $\tan \delta$ peak in QA is about six times larger than that of AR. Above 300°C, the modulus of AR continues to decrease, whereas that of QA increases slightly. The increase is related to relaxation of stress induced in the amorphous material during the quench. Thermal analysis confirms⁹ that the QA film, unlike NEW-TPI amorphous film,^{4,5} did not crystallize significantly upon heating above the T_g .

Effect of Drawing on Draw Ratio and Molecular Extension

AR films were the parent films for the zone-annealing treatment. After drawing, the films were bright yellow and translucent. In all cases, the first draw caused the greatest change in the sample, with subsequent draws increasing the draw ratio only a small amount. The maximum draw ratio was rather low, about 3–4, compared to NEW-TPI, which could be drawn to extensions of 7–8.^{1–3} The limitation in the draw ratio for LARC-CPI is a consequence of using a crystalline starting material, since crystals act as thermoreversible cross-links. Table I lists the draw ratios achieved after multiple stages of zone annealing. The maximum draw ratio vs. number of draws for multiply drawn samples is shown in Figure 3. For a given sample, the draw ratio increases with the number of draws. Figure 4 shows that the maximum draw ratio increases as the maximum drawing temperature increases.

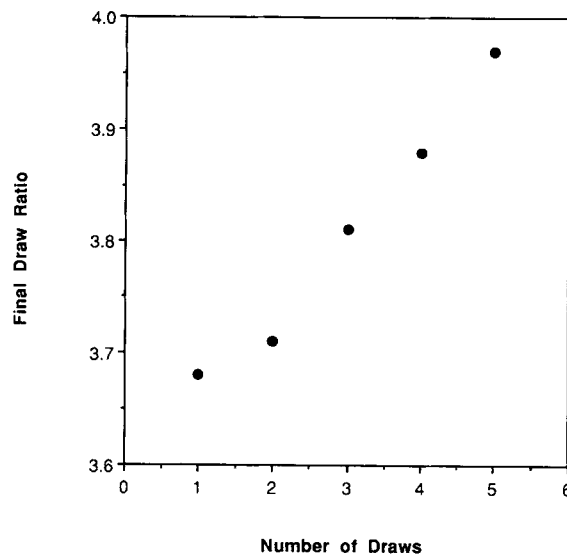


Figure 3 Maximum draw ratio vs. no. draws for zone-annealed LARC-CPI.

The effect of zone annealing on the extension of the amorphous phase network was estimated from a relaxation test. When a sample is stretched, there may be disentanglement and slippage of chains, causing plastic deformation. In addition, there may be elastic deformation that is recovered when the sample is heated. The draw ratio, λ , comprises both types of deformation. To estimate the part of the deformation due to molecular extension, we reheated the drawn film to a temperature just above the drawing temperature to allow relaxation to occur. A test strip of zone-annealed LARC-CPI ($\lambda_{\max} = 3.88$)

Table I Draw Ratio Achieved After Zone Annealing of LARC-CPI at the Indicated Temperatures and Modulus After Final Draw

Sample	Zone-annealing Temperature ^a (°C)					Modulus E' (GPa)
	250	265	280	295	310	
1	3.41	3.46	3.65	3.65	3.72	8.4
2	3.44	3.61	---	---	---	7.6
3	---	3.07	3.46	3.88	---	7.7
4	3.35	3.55	3.57	3.73	3.97	8.5
5	3.61	3.69	3.72	---	---	7.4
6	3.58	---	3.74	---	3.81	9.5
7	---	3.00	3.48	3.65	3.65	7.5
8	3.11	3.35	3.58	3.58	3.58	7.5
9	3.42	---	3.61	---	3.65	9.1
10	---	---	3.63	---	3.71	4.3

^a Sequence of drawing was from low to high temperature.

^b --- indicates the sample was not drawn at this temperature.

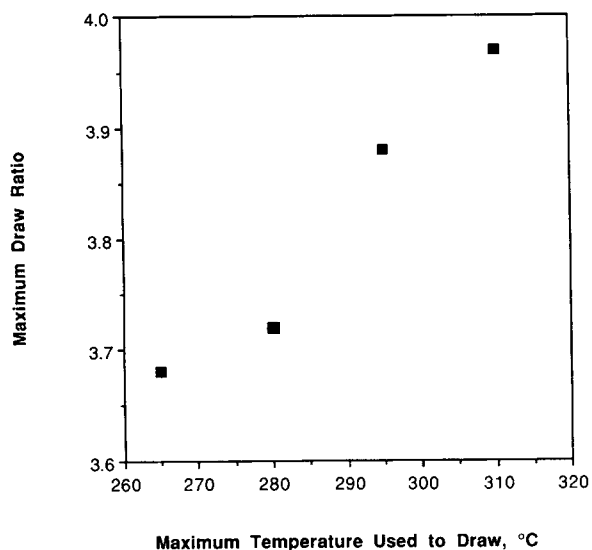


Figure 4 Maximum draw ratio vs. maximum drawing temperature for zone-annealed LARC-CPI.

was heated on a glass slide in an oil droplet so that it could relax unrestricted. It was heated near 300°C for 1 min (this sample had been previously drawn at 295°C), then cooled to room temperature and its length measured. After heating, the sample had shrunk from an extended length, $L_e = 10$ mm, to a shrunk length, $L_s = 6.7$ mm, along the draw direction. The width in the transverse direction was not changed. On the assumption that the recovery of initial deformation is completely elastic, we use the definition of Grubb³³ for molecular extension, M , where

$$M = L_e/L_s = 1.49 \quad (1)$$

The initial network was subject to a molecular extension of 1.49. The remainder of the initial 3.88 extension ratio was due to elastic deformation.

In Figure 1, thermograms of zone-annealed samples, unrelaxed and relaxed, are shown in curves 2 and 3, respectively. Curve 2 is the thermogram of the zone-annealed film that had been drawn to $\lambda_{\max} = 3.88$ and was described in the previous paragraph as the parent film for the relaxation test. Note that there is a clear glass transition relaxation seen in curve 2, and there is a sharp spike in the curve near 260°C. This spike is an artifact (seen in many of the zone-drawn films) that results from contraction of the film inside the DSC pan. Curve 3 is the thermogram of a piece of the same film that had been relaxed as described previously. The relaxed film shows a small T_g step and no artifact. The degrees

of crystallinity of the relaxed ($\chi_c = 0.22$) and unrelaxed ($\chi_c = 0.26$) zone-drawn films are comparable and were always smaller than the degree of crystallinity of the solvent-cast AR film. Thus, the effect of zone annealing the semicrystalline film is to destroy some of the imperfect crystals. In spite of network extension seen in the amorphous phase after drawing, there appears to be no strain-induced crystallization in these films.

The shrinkage, or recovery of the elastic deformation, which we observed also during DSC scanning, occurs as the sample is heated from room temperature to 300°C. Mechanical properties of the drawn films were not stable as a function of temperature, even in the glass region. We found that samples failed at temperatures above the T_g during DMA testing because they were retracting as the elastically deformed amorphous chains returned to their random coil-like configuration.

Effect of Drawing on Crystallite Orientation

As-received LARC-CPI film was semicrystalline and unoriented. The two-dimensional flat-film WAXS pattern is shown in Figure 5. A series of three bright rings is shown and these correspond to the three peaks seen in diffractometer scans shown previously to occur at scattering angles, 2θ , of 18.4°, 22.1°, and 26.8°.^{6,32,34} The spotty ring is from the first reflection (at $2\theta = 28.444^\circ$) of the Si standard powder used for calibration of the ring positions.

The effect of zone annealing is to create highly oriented crystallites and amorphous chains. Orientation of crystallites is shown in Figure 6 (a) and

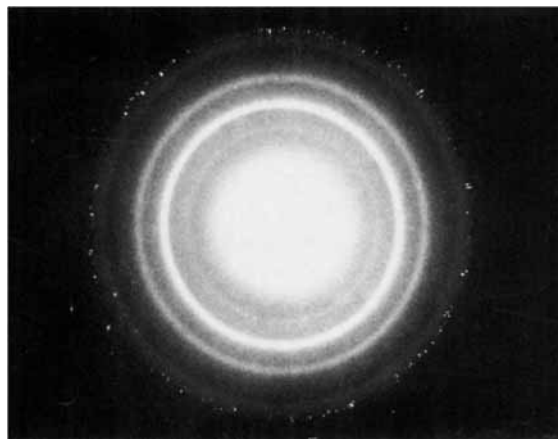


Figure 5 Wide-angle X-ray scattering pattern for as-received LARC-CPI. Spotty ring is from Si powder standard rubbed on the surface of the sample for internal calibration.

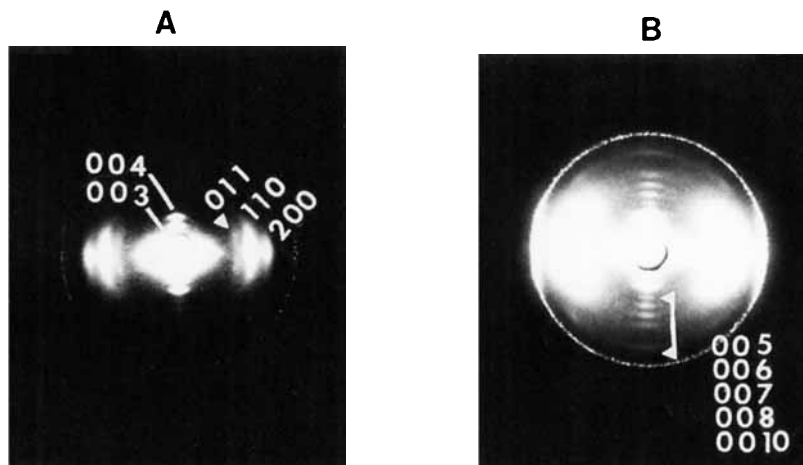


Figure 6 Wide-angle X-ray scattering pattern for zone-annealed LARC-CPI. Fiber axis vertical. Spotty ring from Si powder standard rubbed on the surface of the sample. Sample to film distance about 3 cm: (a) negative exposed to reveal the equatorial reflections; (b) negative overexposed to reveal the meridional reflections.

(b), which is a two-dimensional WAXS fiber pattern of a stack of 12 layers of a zone-annealed film having final draw ratio of 3.72. The fiber axis is vertical, and the spotty ring is from Si. In Figure 6(a), the negative was exposed to reveal the equatorial reflections. In Figure 6(b), the negative was overexposed to reveal the innermost meridional reflections of Miller index type (001). Using a longer sample-to-film distance of about 13 cm, additional meridional reflections can be seen in Figure 7. No silicon ring appears at this distance, so one of the strongest meridional reflections, either (004) or (005) from the pattern of Figure 6, was used to calculate the spacings of the reflections in Figure 7. This reflection occurred on the negative, but is not shown in Figure 7. The positions of the (002), (003), and (004) meridional reflections in Figure 7 matched well with the positions of the same reflections obtained during X-ray experiments at the Brookhaven National Synchrotron Light Source,³⁵ which were calibrated using cholesterol meristate.

The Miller indices were determined by trial-and-error fitting of the positions of the reflections to an assumed structure. Indexing of the fiber pattern was carried out using the reciprocal lattice and Ewald sphere construction. An orthorhombic unit cell structure was assumed, taking into account that the meridional reflections should be of the type (001). Table II lists the proposed Miller indices and the measured d -spacings for 18 reflections. From these reflections, preliminary values for the a -, b -, and c -axis lattice parameters were calculated. We suggest

preliminary values of $a = 8.0 \pm 0.2 \text{ \AA}$, $b = 5.9 \pm 0.2 \text{ \AA}$, and $c = 36.5 \pm 0.3 \text{ \AA}$. The value of the c -axis lattice parameter is very close to the length of the fully extended chain of LARC-CPI determined from CPK models,³⁴ but was not energy-minimized in the present study. In a subsequent effort,^{36,37} we used these preliminary lattice parameters in a molecular modeling study to determine which orthorhombic

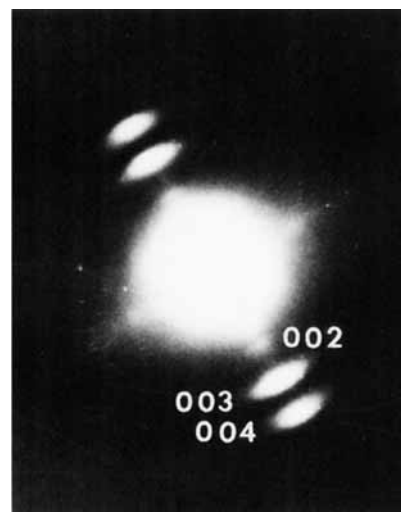


Figure 7 Wide-angle X-ray scattering pattern for zone-annealed LARC-CPI. Fiber axis is along the diagonal, upper left to lower right. Sample to film distance about 13 cm. Negative overexposed to reveal the weak (002) reflection on the meridian.

Table II Miller Indices and *d*-Spacings for X-ray Reflections ($\lambda = 1.54 \text{ \AA}$) in Zone-annealed LARC-CPI

Miller Index	<i>d</i> -Spacing (\AA)
001	36.6
---- ^a	24.5
002	18.0
003	11.9
004	9.3
005	7.1
006	6.1
007	5.3
008	4.6
0010	3.66
010	5.9
011	5.8
110	4.8
020	2.98
200	4.02
210	3.29
220	2.45
124	2.74

^a----This reflection could not be indexed to the assumed orthorhombic unit cell.

cell is correct and to determine the disposition of the chain in the unit cell.

One meridional reflection, occurring at about 24.5 \AA , could not be indexed to the orthorhombic unit cell proposed. At the time of the present study, the origin of this reflection was unknown. In subsequent work,³⁷ we used X-ray photoelectron spectroscopy to show that this reflection comes from oriented diamine segments, most likely from diamine-terminated chain ends that become oriented to produce the meridional reflection at 24.5 \AA .

Mechanical Properties of Drawn LARC-CPI

Figure 8 shows the DMA scans of zone-annealed LARC-CPI. This was one of the few samples that could be successfully measured above T_g , and it was not the sample having the highest modulus. The film was drawn once at 300°C to an approximate draw ratio of 3.7. The glassy modulus of this film is about 3.6 GPa, and E' drops one order of magnitude at T_g , similar to AR film. $\tan \delta$ is asymmetric, being broadened on the high-temperature side.

Many DMA tests failed during the heating attempt to achieve high temperature. As the temperature increased near the T_g , the amorphous chains relax, causing the sample to contract. In addition, the glassy modulus of the materials that displayed

the highest moduli generally decreased as the temperature increased above room temperature. Thus, although the zone annealing of semicrystalline LARC-CPI did result in an increase in glassy storage modulus, the modulus was not stable above room temperature. The reason that the modulus changes even at temperatures far below T_g is related to the method of cooling after the zone-annealing treatment is finished. The films are cooled with the tension force, which consists of a dead weight load, still applied. Therefore, the amorphous phase remains in a nonequilibrium state of stress after the drawing. Further heating during the DMA tests results in the decrease of glassy modulus as a function of temperature as the amorphous phase relaxes.

Dependence of the room-temperature modulus on the number of draws, and on the maximum draw ratio attained, is shown in Figure 9(a) and (b). The modulus of all multiply drawn samples is listed in the last column of Table I. Most of the multiply drawn samples have moduli that are significantly greater than that of undrawn, or once-drawn, LARC-CPI. The limiting modulus achieved in this study appears to be in the range 7.8–9.5 GPa. As the number of draws increases, the highest temperature also increases, since successive draws are conducted at ever-increasing temperatures. Thus, ultimate temperature may be thought to play a role in determining the modulus. However, as seen from Table I, both maximum and minimum values of the modulus were obtained on samples treated at 310°C for the final draw.

The effect of draw ratio on modulus is shown in Figure 9(b). Except for two samples with low moduli, the majority of samples drawn in the range of

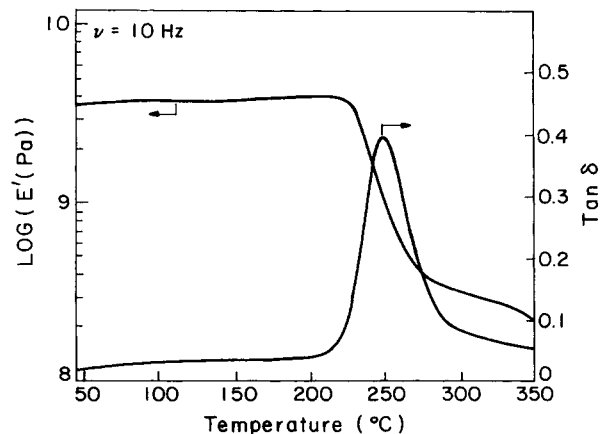


Figure 8 Dynamic mechanical properties, E' and $\tan \delta$, of zone-annealed LARC-CPI as a function of temperature, at 10 Hz.

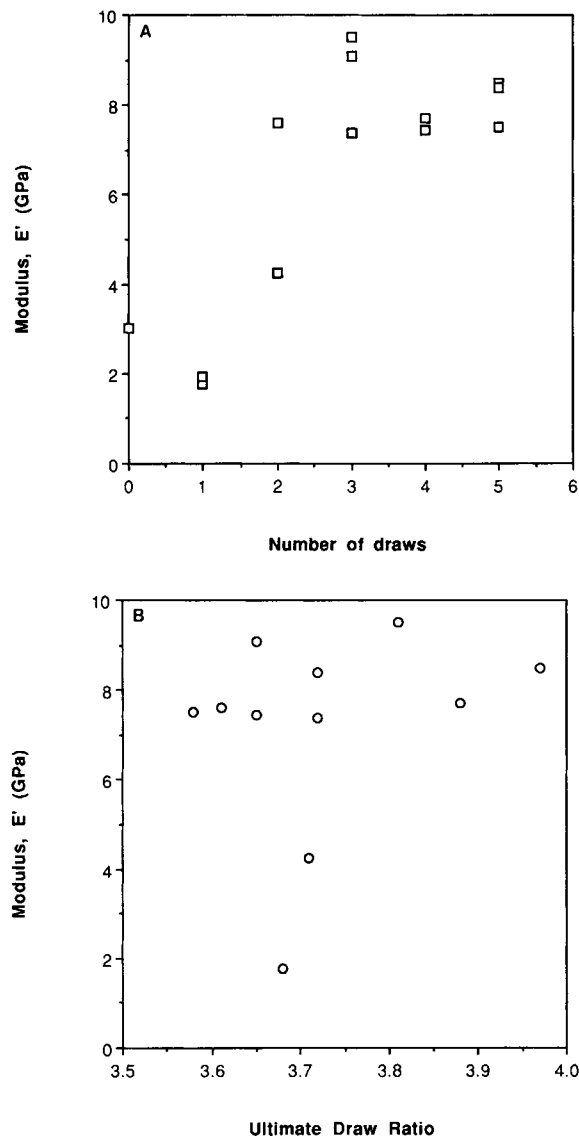


Figure 9 Room-temperature modulus of zone-annealed LARC-CPI vs. (a) no. draws and (b) maximum draw ratio.

$3.5 < \lambda < 4.0$ had similar limiting moduli. We conclude that multiple stages of zone annealing are generally effective in providing a material with high modulus, as long as the drawing conditions result in draw ratios in the range from 3.5 to 4.0.

CONCLUSIONS

Using the zone-annealing treatment on LARC-CPI thermoplastic polyimide, we achieved an increase in the dynamic glassy modulus from about 3.0 GPa (undrawn) to 9.5 GPa ($\lambda = 3.8$). Crystallinity in the parent as-received films limited the ultimate

draw ratio achieved, even when multiple drawing at successively higher temperatures was utilized. The zone-drawn films were highly oriented and were used for X-ray diffraction studies. For the first time, the crystal lattice parameters have been evaluated for LARC-CPI. Preliminary results suggest that LARC-CPI crystals belong to the orthorhombic system and have $a = 8.0 \pm 0.2 \text{ \AA}$, $b = 5.9 \pm 0.2 \text{ \AA}$, and $c = 36.5 \pm 0.3 \text{ \AA}$. Further refinement of these parameters is being undertaken.

This research was supported by NASA Contract NAS1-18846 and the Electric Power Research Institute Contract RP:8007-13.

REFERENCES

1. Y. Aihara and P. Cebe, *ACS Polym. Prepr.*, **33**(1), 471 (1992).
2. Y. Aihara and P. Cebe, *ACS Polym. Prepr.*, **33**(2), 633 (1992).
3. Y. Aihara and P. Cebe, *Polym. Eng. Sci.*, to appear.
4. P. P. Huo and P. Cebe, *Polymer*, **34**(4), 696 (1993).
5. P. P. Huo, J. Friler, and P. Cebe, *Polymer*, **34**(21) 4387 (1993).
6. P. Cebe, J. Friler, J. S. Chung, and P. P. Huo, *SPE Antec*, **37**, 1581 (1991).
7. P. P. Huo, J. Friler, and P. Cebe, *Mater. Res. Soc. Symp. Proc.*, **227**, 239 (1991).
8. J. Friler and P. Cebe, *Polym. Eng. Sci.*, **33**(10), 588 (1993).
9. D. Rich, P. P. Huo, C. Liu, and P. Cebe, *ACS Polym. Mater. Sci. Eng.*, **68**, 124 (1993).
10. J. Friler and P. Cebe, *Mater. Res. Soc. Symp. Proc.*, **214**, 101 (1991).
11. J. B. Teverovsky, MS Thesis, Massachusetts Institute of Technology, 1993.
12. P. M. Hergenrother, N. T. Wakelyn, and S. J. Havens, *J. Polym. Sci. Polym. Chem.*, **25**, 1093 (1987).
13. P. M. Hergenrother and S. J. Havens, *J. Polym. Sci. Polym. Chem.*, **27**, 1161 (1989).
14. P. M. Hergenrother and S. J. Havens, *SAMPE J.*, **24**(4), 13 (1988).
15. P. M. Hergenrother and S. J. Havens, *Polyimides: Material, Chemistry, and Characterization*, Elsevier, Amsterdam, 1989, p. 453.
16. D. Wilson, H. D. Stenzenberger, and P. M. Hergenrother, *Polyimides*, Chapman & Hall, New York, 1990.
17. T. Kunugi, C. Ichinose, and A. Suzuki, *J. Appl. Polym. Sci.*, **31**, 429 (1986).
18. T. Kunugi, A. Mizushima, and T. Hayakawa, *Polym. Commun.*, **27**, 175 (1986).
19. T. Kunugi, S. Oomori, and S. Mikami, *Polymer*, **29**(5), 814 (1988).
20. T. Kunugi, T. Ito, M. Hashimoto, and M. Ooishi, *J. Appl. Polym. Sci.*, **28**, 178 (1983).

21. T. Kunugi, I. Akiyama, and M. Hashimoto, *Polymer*, **23**, 1193 (1982).
22. T. Kunugi, I. Aoki, and M. Hashimoto, *Kobunshi Ronbunshyu*, **38**, 301 (1981).
23. M. Kamezawa, K. Yamada, and M. Takayanagi, *J. Appl. Polym. Sci.*, **24**, 1227 (1979).
24. K. Yamada and M. Takayanagi, *J. Appl. Polym. Sci.*, **27**, 2091 (1979).
25. K. Yamada, M. Kamezawa, and M. Takayanagi, *J. Appl. Polym. Sci.*, **27**, 49 (1981).
26. K. Yamada, M. Oie, and M. Takayanagi, *J. Polym. Sci. Polym. Phys. Ed.*, **21**, 1063-1077 (1983).
27. P. Garrett and D. T. Grubb, *Polym. Commun.*, **29**(3), 60 (1988).
28. P. Garrett and D. T. Grubb, *J. Polym. Sci. Polym. Phys. Ed.*, **26**, 2509 (1988).
29. J. T. Muellerleile and G. Wilkes, *ACS Polym. Prepr.*, **31**(2), 637 (1990).
30. J. T. Muellerleile and G. Wilkes, *Polym. Commun.*, **32**(6), 176 (1991).
31. J. T. Muellerleile, B. G. Risch, D. K. Brandom, and G. Wilkes, *ACS Polym. Prepr.*, **33**(1), 409 (1992).
32. J. T. Muellerleile, B. G. Risch, D. E. Rodrigues, and G. Wilkes, *Polymer*, **34**(4), 789 (1993).
33. D. T. Grubb, *J. Mater. Sci. Lett.*, **3**, 499 (1984).
34. J. B. Friler, MS Thesis, Massachusetts Institute of Technology, 1991.
35. P. Cebe, unpublished data, 1992.
36. M. V. Brillhart, J. B. Teverovsky, J. B. Friler, and P. Cebe, *SPE Antec Tech. Papers*, **40**, 1469 (1994).
37. M. V. Brillhart, Y.-Y. Cheng, P. Nagarkar, and P. Cebe, *Polymer*, to appear.

Received December 1, 1993

Accepted April 21, 1994